Nanoscale Res Lett (2009) 4:210–215
DOI 10.1007/s11671-008-9227-0

NANO EXPRESS

An Effective Amperometric Biosensor Based on Gold Nanoelectrode Arrays

Yanyan Liu · Yingchun Zhu · Yi Zeng · Fangfang Xu

Received: 21 October 2008 / Accepted: 25 November 2008 / Published online: 9 December 2008
© to the authors 2008

Abstract A sensitive amperometric biosensor based on gold nanoelectrode array (NEA) was investigated. The gold nanoelectrode array was fabricated by template-assisted electrodeposition on general electrodes, which shows an ordered well-defined 3D structure of nanowires. The sensitivity of the gold NEA to hydrogen peroxide is 37 times higher than that of the conventional electrode. The linear range of the platinum NEA toward H_2O_2 is from 1×10^{-6} to 1×10^{-2} M, covering four orders of magnitudes with detection limit of 1×10^{-7} M and a single noise ratio (S/N) of four. The enzyme electrode exhibits an excellent response performance to glucose with linear range from 1×10^{-5} to 1×10^{-2} M and a fast response time within 8 s. The Michaelis–Menten constant *k*m and the maximum current density i_{max} of the enzyme electrode were 4.97 mM and 84.60 μA cm^{-2}, respectively. This special nanoelectrode may find potential application in other biosensors based on amperometric signals.

Keywords Gold nanowires · Nanoelectrode arrays · Amperometric biosensor

Y. Liu
Key Lab Special Functional Materials, Henan University, Kaifeng 475004, People's Republic of China

Y. Liu · Y. Zhu (✉) · Y. Zeng · F. Xu
Chinese Academy of Sciences, Key Lab of Inorganic Coating, Shanghai Institute of Ceramics, Dingxi Road, Shanghai 200050, People's Republic of China
e-mail: yzhu@mail.sic.ac.cn; yingchunzhu@yahoo.com

Introduction

Biosensors based on electrochemistry are now attracting considerable attention as potential successors to a wide range of analytical techniques due to their unique properties of specificity [1–3]. The key aspect of an electrochemical biosensor is the generation or modulation of electrical current in an electronic circuit between the bioreaction or bio-recognition systems and the electronic elements. The high demand for selection and sensation requires not only the appropriate biological macromolecules with high active, but also the suitable substrates with biocompatible surroundings and efficient transport of electrons, but it is difficult for conventional electrodes to satisfy the demands. To that end, specific materials and structures with novel biocompatibility, stability, and electron transport property are demanded, for example, the intensively investigated nanomaterials [4, 5].

Nanomaterials, especially the one-dimensional nanostructures such as carbon nanotubes (CNT) [6] and metal [7], semiconductor [8], or conducting polymer [9] nanowires or nanotubes, are particularly attractive for biosensor application due to their unique advantages including high surface-to-volume ratio, elevated electrochemical activity, and eminent electron communication features. Usually, nanotubes and nanowires are incorporated into the functional systems by a variety of methods, such as solution evaporation [10], sol–gel encapsulation [11], and polymer-assisted dispersion [12]. These methods generally result in disarrayed and layered films with the absorbed catalytic enzyme sites partially blocked and the substrate transport to the enzymes hindered [13], leading to a low amperometric responses upon bio-electrocatalysed oxidation or reduction of the analyte. To overcome this problem, perpendicularly aligned nanotube or nanowire arrays can be

formed as sensing devices [7, 14, 15], which will lead to an increment of enzyme content associated with the electrode surface, an improvement of electrical communication between the redox center and the electrode, and thus an enhancement of the transduced amperometric signal.

Metal gold is one of the mostly used noble metals in biosensors; several reports have demonstrated that gold nanoparticles may be used as a hopping bridge of electrons generated from the enzyme catalytic redox reaction [16–18]. Besides facilitating the transfer of electrons, gold nanoparticles can also provide a biocompatible environment for proteins, since they are not toxic to the biological systems [19, 20]. Gold nanoparticles are an excellent candidate for replacing potentially harmful mediators in the construction of biosensors.

In this paper, we fabricated the gold nanoelectrode array (NEA) in the template of polycarbonate (PC) membranes. Free standing nanostructured gold nanowire arrays were obtained by direct electrodepositing on the conventional gold electrode, analogous to ultramicroelectrode ensembles reported by Penner et al. [21]. The whole system can be considered as a modified electrode consisting of millions of nanowires which contact well with the substrate electrode; the diameter of each nanowire is about 450 nm and the length is even 4 μm. The 3D nanowire array results in large electroactive surface area, which is about five times as large as the conventional gold electrode. The high electroactive surface can not only enhance the sensitivity to hydrogen peroxide, but also provide large space for the loading of the enzymes. Considering the advantages of NEA and biocompatibility of metal gold, we put the gold NEA into the use of enzymes biosensors, which showed high sensitivity and wide linear range.

Experimental

Reagents and Measurements

The track-etch polycarbonate membranes (PC membranes) with a pore diameter of 450 nm as template were purchased from Whatman (USA), the plating agent of gold sodium sulfite ($Na_3Au(SO_3)_2$, 50 g/L) was provided by Changzhou Chemical Research Institute, sodium sulfite (Na_2SO_3, 99.5%), sodium hydroxide (NaOH, 99.5%), dichloromethane (CH_2Cl_2, 99.5%), potassium hexacyanoferrate (III) ($K_3Fe(CN)_6$, 99.5%), potassium hexacyanoferrate (II) ($K_4Fe(CN)_6$, 99.5%), bovine serum albumin (BSA), glutaraldehyde (25%) and D(+)-glucose (99.5%) were all purchased from Sinopharm Chemical Reagent Co., Ltd, China, and glucose oxidase (GOD, EC 1.1.3.4, from Aspergillus niger, 15,200 units/g solid) was bought from Sigma. A 1/15 M phosphate buffer (PB, pH 6.98) solution which prepared using Na_2HPO_4 and KH_2PO_4 was employed as supporting electrolyte during the electrochemical measurements. All other chemicals were reagent grade and all solutions were prepared from double-distilled water.

The cyclic voltammetry (CV) measurements and amperometric response measurements of NEA was performed on a Solartron electrochemical interface (Model 1287) while the electrochemical impedance spectrum (EIS) measurements were carried out on the Solartron impedance/gain-phase analyzer (Model 1260). A conventional three-electrode system was used in all the above measurements. NEA and NEA/GOD were used as working electrode, Ag/AgCl was used as reference electrode, and a spiral platinum wire acted as a counter electrode. The CVs and EISs were recorded in 5 mM $[Fe(CN)_6]^{3-/4-}$ containing 0.1 M KCl. The potential amplitude was kept as 10 mV and the measured frequency range was 10^{-1}–10^5 Hz in EIS experiments. All measurements were carried out at room temperature.

Deposition of Gold Nanowire Arrays on Electrodes

For the electrodeposition of Au nanowire array, a convex Au-disk electrode ($R = 3$ mm) was used as the substrate electrodes. Well substrate surface/membrane contact is achieved with convex substrate electrodes than with conventional planar electrodes [21]. A porous host PC membrane was attached onto the surface of an Au-disk electrode ($R = 3$ mm) and then fixed with a Teflon O-ring (Fig. 1). Electrodeposition was performed using galvanostat method with the PC membrane/Au electrode as working electrode and a spiral platinum wire as counter electrode. The electroplating solution is 5 g L^{-1} $Na_3Au(SO_3)_2$ solution containing 40 g L^{-1} Na_2SO_3 and 4 g L^{-1} NaOH, and the current density is 0.01 A dm^{-2}. After deposition, the PC template was dissolved by immersion of the electrode in chloroform.

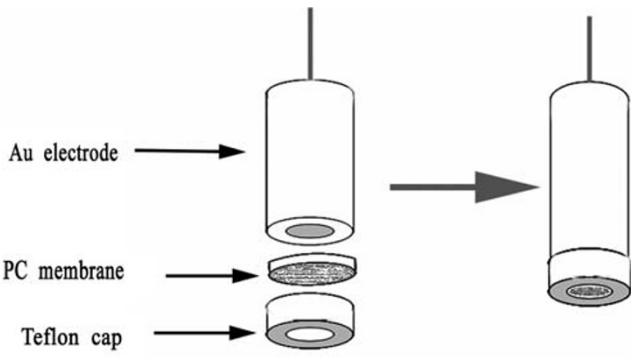

Fig. 1 Immobilization of PC membrane on Au electrode

Immobilizing GOx on the Gold NEA Electrode

Before modification, the NEA was washed successively using Piranha (3:1 v/v mixture of concentrated H_2SO_4 and H_2O_2), ethanol, and water. The GOD was immobilized on the NEA and Au electrodes by first forming a GOD/BSA solution comprising of glucose oxidase (10 mg/ml) and bovine serum albumin (5 mg/ml) dissolved in buffer. Then 2 μL glutaraldehyde was added to 10 μL GOD/BSA solution and mixed rapidly. About 3 μL of the intermixture was cast onto the electrode, and air dried at 4 °C.

Results and Discussion

Morphologicl and Electrochemical Characterization of the Gold Nanowire Array Electrode

At the first stage, gold was electrodeposited on the electrode surface and the color of the PC membrane kept white until the space between the membrane and the electrode surface is filled. Then, the gold was electrodeposited in the pores of the membrane forming nanowire arrays, and the color of the membrane changed into yellow. Figure 2 shows the SEM images of the gold NEA after 50 min deposition; it can be seen that the whole array is consisted of millions of free standing nanowires, and the surface density of the nanowires is calculated to be $8 \times 10^7/\text{cm}^2$. The nanowires are highly regular and uniform, with an average diameter of 450 nm and length of 4 μm. Each nanowire stands straightly on the substrate, shows a nice contact between the nanowire and the substrate electrode. We have tried different deposition time for the preparation of the nanowire electrode. Short nanowires with an average diameter of 450 nm are obtained when shorter deposition time is employed, which leads to a lower electroactive surface area. The nanowire arrays will be covered by gold coating when over-deposition is carried out.

Figure 3 represents cyclic voltammograms (CVs) of the conventional Au-disk electrode (a) and the gold NEA grown on the Au electrode in 5 mM $[Fe(CN)_6]^{3-/4-}$ containing 0.1 M KCl at scan rate of 50 mV/s. The well-defined oxidation and reduction peaks at +0.30 and +0.17 V versus Ag/AgCl due to the Fe^{3+}/Fe^{2+} redox couple in forward and reverse scans, respectively. The peak current (i_{pa} or i_{pc}) can be expressed by the Randles–Sevcik equation [22] as shown in Eq. 1:

$$i_p = 0.4463\, nFAC(nFvD/RT)^{1/2} \quad (1)$$

where i_p (A) is the peak current, n the number of electrons appearing in half-reaction for the redox couple, F the Faraday's constant (96,485 C mol^{-1}), A the electrode area (cm^2), v the rate at which the potential is swept (V s^{-1}), D the analyte's diffusion coefficient (cm^2 s^{-1}), R the universal gas constant (8.314 J mol^{-1} K^{-1}), C the molar concentration of analyte (mole cm^{-3}), and T is the absolute temperature (K). The electroactive surface area (A) is a linear function of the peak current of the redox couple. As shown in Fig. 3, redox peak current of gold NEA is 5.0 mA cm^{-2}, which is about five times of the conventional Au electrode (1.0 mA cm^{-2}). Therefore, the average value of the electroactive surface area of the NEA was about five times as large as the conventional Au electrode.

Detection of Hydrogen Peroxide with the Gold NEA Electrode

Experiments were performed to determine the electrochemical response of H_2O_2 at the NEA electrode and the conventional Au electrode, respectively. Figure 4 shows the current–time response of the conventional gold electrode and the gold NEA at +0.6 V versus Ag/AgCl in a stirred solution for successive addition of 1 mM H_2O_2; the right insert in Fig. 4 shows current–time response of the gold NEA for the successive addition of 1 μM H_2O_2. Fast response can be observed at the two electrodes with

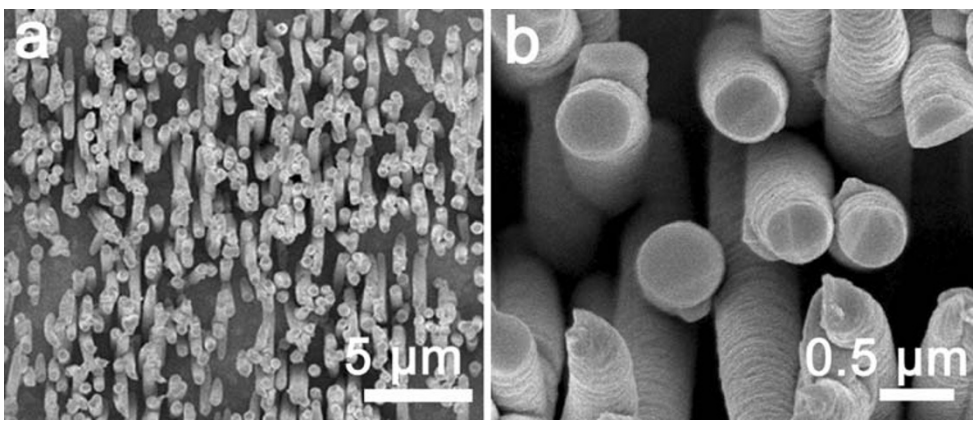

Fig. 2 SEM images of the gold nanowire array on the electrode

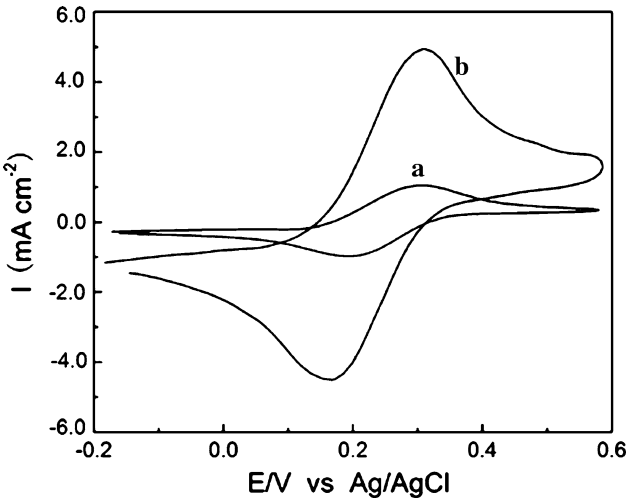

Fig. 3 Cyclic voltammograms (CVs) of **a** conventional Au electrode and **b** gold NEA in 5 mM $[Fe(CN)_6]^{3-/4-}$ containing 0.1 M KCl. Scan rate, 50 mV s^{-1}

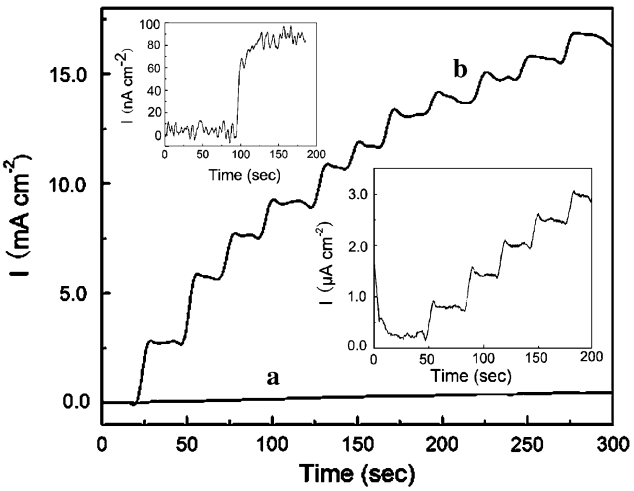

Fig. 4 Current–time curve of the conventional gold electrode (**a**) and gold NEA (**b**) to the successive addition of 1 mM hydrogen peroxide at 0.6 V in PB. The insert (right) shows current–time curve of the gold NEA to the successive addition of 1 μM hydrogen peroxide. The insert (left) shows detection limit of 100 nM with S/N = 4

steady-state current reached within 5 s. The sensitivity of the gold NEA to H_2O_2 is 1.52 mA mM^{-1} cm^{-2}, which is 37 times higher than that of the conventional electrode (0.04 mA mM^{-1} cm^{-2}), indicating high catalytic activity of the gold NEA to hydrogen peroxide. The linear range of the gold NEA to H_2O_2 is from 1×10^{-6} to 1×10^{-2} M, covering four orders of magnitudes with a detection limit of 1×10^{-7} M with S/N = 4 (left insert in Fig. 4). This reveals that the electrodeposited nanowire array electrodes show high sensitivity, wide linear range, and low detection limit to hydrogen peroxide in comparison with conventional electrodes and gold nanostructures immobilized electrodes [7] due to the excellent conductivity and activity. The gold NEA electrode shows excellent stable performance on measuring hydrogen peroxide, and no apparent signal change is found after 4 month storage.

Electrochemical Impedance Spectrum Analysis of the GOD/NEA Enzyme Electrode

Electrochemical impedance spectroscopy (EIS) is an effective tool to study processes in the interfacial region of the electrode systems, especially to modified surfaces, and is frequently used for realizing electrochemical transformation and processes associated with conductive supports [23, 24]. Figure 5 illustrates the results of EIS in the form of Nyquist plots on Au/GOD electrode and NEA/GOD electrode using $[Fe(CN)_6]^{3-/4-}$ as the redox probe. The curve of the EIS includes a semicircular part and a linear part. The semicircular part at higher frequencies corresponds to the electron-transfer limited process, which controls the electron-transfer kinetics of the redox probe at the electrode interface. Meanwhile, the linear part at lower frequencies corresponds to the diffusion process [25]. Based on this fact, traditional Randles electrical circuits (Fig. 6.) was chose for EIS fitting [26]. The circuit includes the ohmic resistance of the electrolyte solution (R_s), the Warburg impedance (W), resulting from ion diffusion from the bulk electrolyte to the electrode interface, the constant phase element (CPE), and charge-transfer resistance (R_{ct}). Here, considering the influence of the surface roughness,

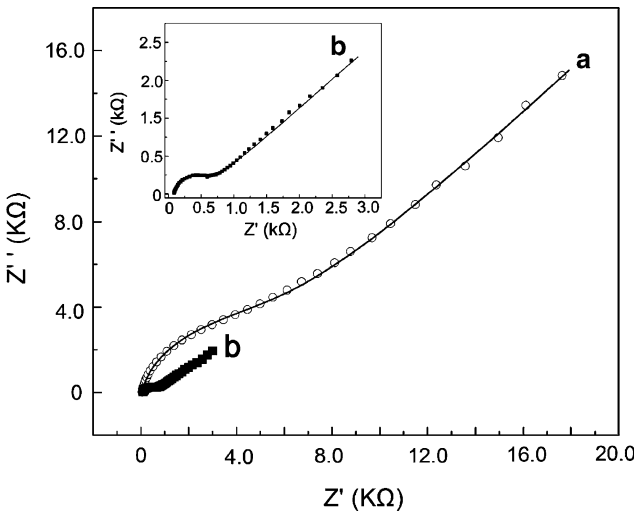

Fig. 5 EIS curves of **a** Au/GOD electrode (◯), **b** NEA/GOD electrode (■) in the 5 mM $[Fe(CN)_6]^{3-/4-}$ solution containing 0.1 M KCl. The real line in both (**a**) and (**b**) are the simulated curves (calculated based on the equivalent electrical circuit in Fig. 6), the insert is the magnified view of **b**)

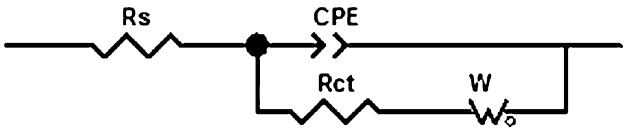

Fig. 6 Equivalent electrical circuits simulated in Fig. 5

CPE (constant phase element) is used to describe the double layer capacitance, instead of the pure capacitance.

The simulated curves based on the equivalent electrical circuit in Fig. 6 fit well with the experimental EIS spectra. The R_{ct} of the NEA/GOD electrode is 453 Ω, which is apparently smaller than that of the Au/GOD electrode (3,362 Ω). The CPE of the NEA/GOD electrode is 3.1 μF, which is smaller than that of the Au/GOD electrode (4.9 μF). This can be ascribed to the structural difference of the electrodes. The surface of the bare Au electrode is flat, which can be described as two dimensions, while the nanowire array electrode fills three dimensions. The GOD spread as a compact film on the bare Au electrode, while it can fill in the space of nanowires on the NEA electrode. The gold nanowires effectively improved the conductivity of the NEA/GOD electrode and thus decreased the charge-transfer resistance. The special structure of the NEA/GOD electrode also led to a small CPE. The EIS analysis indicates that the three-dimensional structure of the NEA/GOD electrode is advantageous for the charge-transfer, which is an excellent characteristic for amperometric biosensors.

Glucose Detection with the GOD/NEA Enzyme Electrode

Figure 7a illustrates a typical current–time plot for the GOD modified NEA upon the successive addition of glucose at 0.60 V. It can be observed that, the response current increased with increasing the concentration of glucose and finally reached a steady-state value. A response time of about 8 s was obtained. Such a fast response time can be attributed to the 3D oriented nanowire array structures and the favorable biocompatibility of gold. Figure 7b shows the calibration curve of glucose at the enzyme electrode. The enzyme electrode gave a linear response to glucose in the range from 1×10^{-5} to 1×10^{-2} M and detection limit of 5×10^{-6} M was obtained based on S/N = 3 (Fig. 7a, insert). This result is better than that of the GOD-immobilized Au nanoparticles-modified electrode [27, 28].

Since the electrode responses were a kinetic process, the apparent Michaelis–Menten constant (k_m) and the maximum current density (i_{max}) can be obtained by an amperometric method as suggested by Shu and Wilson [29] as shown in Eq. 2:

$$\frac{1}{i_s} = \frac{k_m}{i_{max}} \times \left(\frac{1}{C_g}\right) + \frac{1}{i_{max}} \quad (2)$$

where i_s is the steady-state current, C_g is the concentration of glucose, k_m is the apparent Michaelis–Menten constant and i_{max} is the maximum current. From the curve of the ${i_s}^{-1}$ versus ${C_g}^{-1}$, based on the experimental data from Fig. 7b, the apparent Michaelis–Menten constant k_m and the maximum current density i_{max} were estimated to be 4.97 mM and 84.60 μA cm^{-2}. The small k_m means that the immobilized GO_x possesses a high enzymatic activity and the proposed electrode exhibits a high affinity for glucose [30]. The GOD/NEA enzyme electrode also shows high stability for glucose detection, which retains about 80% of its original response after 3 months of storage. The decrease of response to glucose may be due to the loss of the activity of the immobilized glucose oxidase, since the gold NEA electrode shows excellent stable performance on measuring hydrogen peroxide.

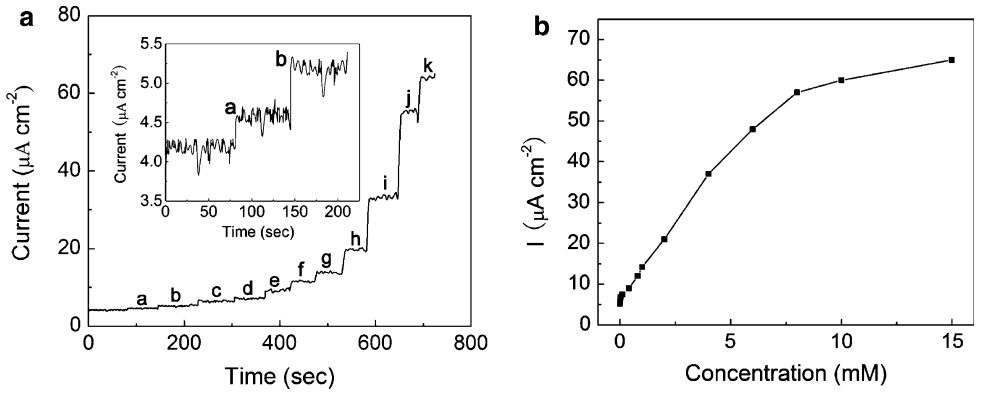

Fig. 7 **a** Response currents of the Au NEA/GO_x electrode to injection of glucose into a stirred phosphate buffer (pH 6.9) at 0.60 V. Final concentrations: (a) 5×10^{-6} M (b) 1×10^{-5} M (c) 2×10^{-5} M, (d) 1×10^{-4} M, (e) 4×10^{-4} M, (f) 8×10^{-4} M, (g) 1×10^{-3} M, (h) 2×10^{-3} M, (i) 4×10^{-3} M, (j) 8×10^{-3} M, (k) 1×10^{-2} M. Inset shows a magnification of the first three additions of glucose. (S/N = 3). **b** Calibration curve of the GOD modified gold NEA toward glucose

Conclusion

In this work, we prepared a novel gold NEA that shows better electrochemical properties than conventional Au electrode. Biosensors based on this nanostructure have improved analytical performances compared to the conventional electrode. Specifically, the biosensor shows a wider linear response to glucose in the range from 1×10^{-5} to 1×10^{-2} M and a higher maximum current density. A fast response time within 8 s and a very high response current density of 84.60 μA cm^{-2} were achieved. The apparent ichaelis–Menten constant of 4.97 mM also shows good affinity to glucose. The above facts indicate that the gold nanowire array electrode may be also used in the fabrication of other biosensors based on oxidases, such as biosensors for choline, cholesterol, and alcohol.

Acknowledgment The research was partially financially supported from the Nation Natural Science of China (20571082, 50772125), the Science and Technology Commission of Shanghai (08JC1420700), and the National High Technology Research and Development Program of China.

References

1. A.K. Wanekaya, W. Chen, N.V. Myuang, A. Mulchandani, Electroanalysis **18**, 533 (2006). doi:10.1002/elan.200503449
2. L. Murphy, Curr. Opin. Chem. Biol. **10**, 177 (2006). doi:10.1016/j.cbpa.2006.02.023
3. W. Zhao, J.J. Xu, H.Y. Chen, Electroanalysis **18**, 1737 (2006). doi:10.1002/elan.200603630
4. J. Wang, Analyst (Lond) **130**, 421 (2005). doi:10.1039/b414248a
5. E. Katz, I. Willner, J. Wang, Electroanalysis **16**, 19 (2004). doi:10.1002/elan.200302930
6. D.H. Jung, B.H. Kim, Y.K. Ko, M.S. Jung, S. Jung, S.Y. Lee, H.T. Jung, Langmuir **20**, 8886 (2004). doi:10.1021/la0485778
7. M. Delvaux, A. Walcarius, S. Demoustier-Champagne, Anal. Chim. Acta **525**, 221 (2004). doi:10.1016/j.aca.2004.08.054
8. F.F. Zhang, X.L. Wang, S.Y. Ai, Z.D. Sun, Q. Wan, Z.Q. Zhu, Y.Z. Xian, L.T. Jin, K. Yamamoto, Anal. Chim. Acta **519**, 155 (2004). doi:10.1016/j.aca.2004.05.070
9. H.H. Zhou, H. Chen, S.L. Luo, J.H. Chen, W.Z. Wei, Y.F. Kuang, Biosens. Bioelectron. **20**, 1305 (2005). doi:10.1016/j.bios.2004.04.024
10. Z.H. Gan, Q. Zhao, Z.N. Gu, Q.K. Zhuang, Anal. Chim. Acta **511**, 239 (2004). doi:10.1016/j.aca.2004.01.055
11. Y. Lin, S. Taylor, H.P. Li, K.A. Shiral Fernando, L.W. Qu, W. Wang, L.R. Gu, B. Zhou, Y.P. Sun, J. Mater. Chem. **14**, 527 (2004). doi:10.1039/b314481j
12. J. Wang, M. Musameh, Y.H. Lin, J. Am. Chem. Soc. **125**, 2408 (2003). doi:10.1021/ja028951v
13. J. Wang, M. Scampicchio, R. Laocharoensuk, F. Valentini, O. Gonz lez-Garcýá, J. Burdick, J. Am. Chem. Soc. **128**, 4562 (2006). doi:10.1021/ja061070u
14. M. Delvaux, S. Demoustier-Champagne, Biosens. Bioelectron. **18**, 943 (2003). doi:10.1016/S0956-5663(02)00209-9
15. S. Sotiropoulou, N.A. Chaniotakis, Anal. Bioanal. Chem. **375**, 103 (2003)
16. Y. Xiao, F. Patolsky, E. Katz, J.F. Hainfeld, I. Willner, Science **299**, 1877 (2003). doi:10.1126/science.1080664
17. S. Bharathi, M. Nogami, S. Ikeda, Langmuir **17**, 1 (2001). doi:10.1021/la0010572
18. J. Zhao, A.L. O'Daly, R.W. Henkens, J. Stonehurner, A.L. Crumbliss, Biosens. Bioelectron. **11**, 493 (1996). doi:10.1016/0956-5663(96)86786-8
19. X. Chen, J. Li, X. Li, L. Jiang, Biochem. Biophys. Res. Commun. **245**, 352 (1998). doi:10.1006/bbrc.1998.8431
20. Y. Xiao, H. Ju, H. Chen, Anal. Chim. Acta **391**, 73 (1999). doi:10.1016/S0003-2670(99)00196-8
21. R.M. Penner, C.R. Martin, Anal. Chem. **59**, 2625 (1987). doi:10.1021/ac00148a020
22. J.E.B. Randles, Trans. Faraday Soc. **44**, 327–338 (1948). doi:10.1039/tf9484400327
23. J.J. Feng, J.J. Xu, H.Y. Chen, J. Electroanal. Chem. **585**, 44 (2005). doi:10.1016/j.jelechem.2005.07.010
24. S. Komaba, T. Osaka, J. Electroanal. Chem. **453**, 19 (1998). doi:10.1016/S0022-0728(97)00238-6
25. H.L. Zhang, X.Z. Zou, G.S. Lai, D.Y. Han, F. Wang, Electroanalysis **19**, 1869 (2007). doi:10.1002/elan.200703942
26. J.E.B. Randles, Discuss. Faraday Soc. **1**, 11 (1947)
27. Y.G. Liu, X.M. Feng, J.M. Shen, J.J. Zhu, W.H. Hou, J. Phys. Chem. B **112**, 9237 (2008). doi:10.1021/jp801938w
28. B.-Y. Wu, S.-H. Hou, F. Yin, J. Li, Z.-X. Zhao, J.-D. Huang, Q. Chen, Biosens. Bioelectron. **22**, 838 (2007). doi:10.1016/j.bios.2006.03.009
29. F.R. Shu, G.S. Wilson, Anal. Chem. **48**, 1679 (1976). doi:10.1021/ac50006a014
30. B. Wang, B. Li, Q. Deng, S. Dong, Anal. Chem. **70**, 3170 (1998). doi:10.1021/ac980160h